Precursory accelerated Benioff strain in the Aegean area

Costas Papazachos and Basil Papazachos
Geophysical Laboratory, University of Thessaloniki, Greece

Abstract
Accelerating seismic crustal deformation due to the occurrence of intermediate magnitude earthquakes leading to the generation of a mainshock has recently been considered a critical phenomenon. This hypothesis is tested by the use of a large data sample concerning the Aegean area. Elliptical critical regions for fifty-two strong mainshocks, which have occurred in the Aegean area since 1930, have been identified by applying a power-law relation between the cumulative Benioff strain and the time to the main rupture. Empirical relations between the parameters of this model have been further improved by the use of a large data sample. The spatial distribution of preshocks with respect to the mainshock is examined and its tectonic significance is pointed out. The possibility of using the results of this work to predict the epicentre, magnitude and time of ensuing mainshocks are discussed and further work towards this goal is suggested.

Key words *Benioff strain – critical point – Aegean area*

1. Introduction

Seismological observations of the last four decades have shown that large earthquakes follow periods of accelerating regional intermediate magnitude seismicity (Tocher, 1959; Mogi, 1969; Raleigh *et al.*, 1982; Papadopoulos, 1986; Varnes, 1989; Sykes and Jaume, 1990; Knopoff *et al.*, 1996). It has been further shown that the time variation of measures of seismic deformation (seismic moment, Benioff strain, etc.) follows a power-law predicted by statistical physics if we consider the process of generation of these moderate-magnitude shocks (preshocks) a critical phenomenon and the large earthquake (mainshock) a critical point (Sornette and Sornette, 1990; Allerge and Le Mouël, 1994; Andersen *et al.*, 1997). The term preshock does not indicate only the classical foreshocks but the long-term sequence of moderate-magnitude events that occur in a broad area, leading to the generation of the large event. Thus, Bufe and Varnes (1993) used the cumulative Benioff strain, $S(t)$, as a measure of the preshock seismicity at time t, defined as

$$S(t) = \sum_{i=1}^{n(t)} E_i(t)^{1/2} \qquad (1.1)$$

where E_i is the seismic energy of the ith preshock and $n(t)$ is the number of events at time t. To fit the time variation of the cumulative Benioff strain they proposed a relation of the form

$$S(t) = A + B(t_c - t)^m \qquad (1.2)$$

where t_c is the origin time of the mainshock and A, B, m are parameters that can be calculated by the available data. The seismic energy required in relation (1.1) is calculated by formulas, which relate this energy to the magnitude of the earthquakes.

Mailing address: Prof. Costas Papazachos, Geophysical Laboratory, University of Thessaloniki, P.O. Box 352-1, GR-54 006, Thessaloniki, Greece; e-mail: costas@lemnos.geo.auth.gr

Bowman *et al.* (1998) applied a procedure to identify circular regions approaching criticality before mainshocks of $M \geq 6.5$ that occurred along the San Andreas fault system since 1950 by minimizing a curvature parameter, C, which quantifies the degree of acceleration of the Benioff strain. They defined this parameter as the ratio of the root-mean square error of the power law fit (relation (1.2)) to the corresponding linear fit error. Thus, C is less than 1 for accelerating or decelerating seismicity and equals 1 for a linear variation of seismicity with time.

Papazachos and Papazachos (2000) applied the criterion of minimum C value to identify elliptical regions in the Aegean area where seismicity was accelerated before twenty-four shallow strong mainshocks (M = 6.0-7.5) that occurred between 1948 and 1997. In their study they showed a clear accelerated seismic energy release behaviour in all the studied preshock sequences, in very good agreement with the pattern described by eq. (1.2). They also defined a linear relation between the radius, R (in km), of the circle that has an area equal to the corresponding elliptical region and the magnitude, M, of the mainshock, as well as a linear relation between the logarithm of the duration of the accelerating seismicity, t_p (in years), and the rate of the Benioff strain release, s_r (in Joule$^{1/2}$ per year and per 10000 km^2). Furthermore, Papazachos and Papazachos (2001) used the data for the twenty-four mainshocks in the Aegean area mentioned above to define three additional relations, which can be used for independent estimations of parameters of the relation (1.2). They showed that the parameter A is equal to the product of the long term mean rate of the Benioff strain, S_r (in Joule$^{1/2}$/yr), in the corresponding preshock region and the preshock time, t_p (in years), while the logarithm of the parameter B is a linear function of the magnitude of the mainshock. They have further shown that the mainshock magnitude is a linear function of the average magnitude, M_{13}, of the three largest preshocks of each preshock sequence.

Very recently, Papazachos *et al.* (2000) published a new catalogue of earthquakes for Greece and surrounding area that includes information for a significantly larger number of earthquakes (20580 shocks) than previous catalogues. Thus, it is now possible to use this catalogue to investigate more preshock sequences in this area and to use more data for identifying and studying each of these sequences. Therefore, the first target of this paper is to investigate the properties of a relatively large number of preshock sequences in the Aegean area (52 sequences) and to further improve the relations between the parameters of the relation (1.2), which describe the model followed by the preshock-mainshock sequences. The second target of the paper is to use the result for these 52 preshock-mainshock sequences to define the spatial distribution of preshocks of each sequence with respect to the epicentre of the corresponding mainshock and to search for any tectonic implication of this distribution. Such results, in addition to their theoretical (tectonic) implications, are of great practical importance because they can be used to predict the epicentre of the mainshock when the preshock region has been identified.

The Aegean area, which is the main study area, is seismically the most active part of the whole western Eurasia. It is formed by the Hellenic arc (fig. 1), where convergence takes place between Eurasia and Africa and by the Aegean sea, which is a marginal sea where mainly expansions take place. There is also a long transtensional zone along the North Aegean trough, which separates the Aegean from the Eurasian plate, where mainly strike slip faulting takes place. The high seismicity of the area and the strongly spatially varying geotectonic setting suggest that the Aegean area is an appropriate «test site» for the evaluation of the hypothesis adopted in the present paper.

2. Data and method

The catalogue for earthquakes in the Aegean and surrounding area (34°N-43°N, 19°E-30°E) includes historical and instrumental data with $M \geq 4.0$ (Papazachos *et al.*, 2000). In the present paper only instrumental data are used, which have been available since 1911 when the first modern seismograph was put into regular operation in this area (a two-component horizontal

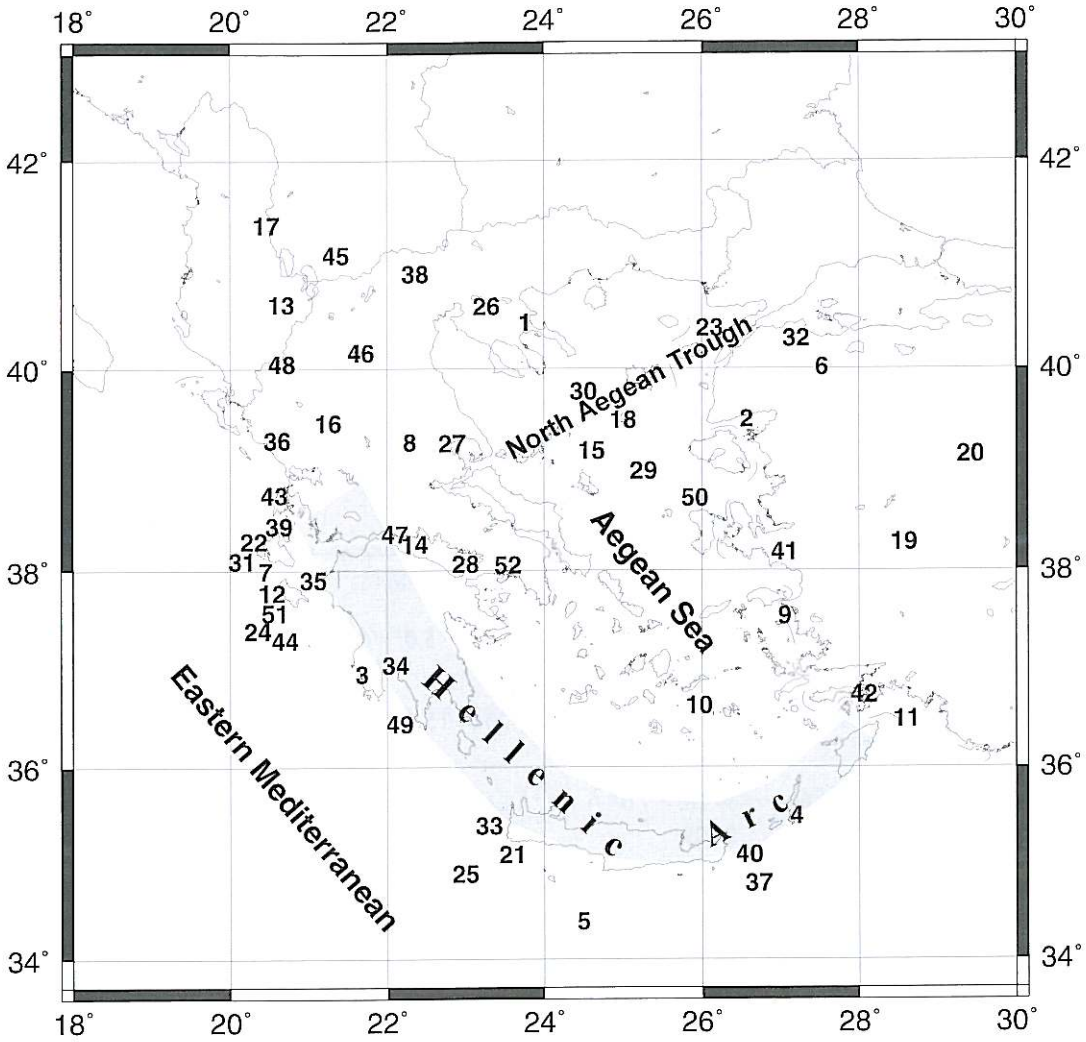

Fig. 1. Epicenters of the fifty-two shallow mainshocks for which preshock critical regions have been determined.

Mainka seismograph in Athens). The instrumental data included in this catalogue are complete for $M \geq 5.0$ during 1911-1999, $M \geq 4.5$ during 1950-1999, $M \geq 4.3$ during 1965-1999 and $M \geq 4.0$ during 1981-1999. Only complete data are used in the present study. The typical standard error in the epicentres varies with time and magnitude and is of the order of 15 km for earthquakes after 1965 (when the first network of stations was established in this area) and around 25 km for older earthquakes ($M \geq 5.0$ for 1911-1949 and $M \geq 4.5$ for 1950-1964). All magnitudes are equivalent moment magnitudes; either originally reported or converted from other magnitude scales by appropriate formulas (Papazachos *et al.*, 1997; Margaris and Papazachos, 1999) and their corresponding errors can be up to 0.3.

Table I. Information on the 52 mainshocks (code number N, date, origin time, epicentre, magnitude) and on the preshocks (number of preshock n-1, preshock duration, t_p (in years), minimum preshock magnitude, M_{min}, average magnitude, M_{13}, of the three largest preshocks, average time difference, t_{13}, between the three largest preshocks and the mainshock, the mean epicentre of preshocks and the length, x (in km), and the azimuth, ξ (in degrees), of the vector that starts at the mean preshock epicentre and ends at the mainshock epicentre.

N	Date	h:min:s	φ°_{N}, λ°_{E}	M	n	t_p	M_{min}	M_{13}	t_{13}	φ°_{N}, λ°_{E}	x	ξ
1	1932, 09, 26	19:20:42	40.45, 23.76	7.0	41	21.7	5.0	6.4	4.3	39.91, 23.54	63	17
2	1944, 10, 06	02:34:41	39.51, 26.57	7.0	42	24.8	5.0	6.4	8.2	39.47, 27.25	59	274
3	1947, 10, 06	19:55:34	36.96, 21.68	7.0	45	19.8	5.0	6.2	3.8	37.42, 21.37	58	151
4	1948, 02, 09	12:58:13	35.50, 27.20	7.1	55	21.1	5.0	6.1	6.9	35.47, 26.87	30	84
5	1952, 12, 17	23:03:57	34.40, 24.50	7.0	43	34.0	5.0	6.0	11.5	34.71, 24.41	36	166
6	1953, 03, 18	19:06:16	40.02, 27.53	7.4	44	33.2	5.0	6.7	8.5	39.44, 27.40	66	10
7	1953, 08, 12	09:23:52	38.00, 20.35	7.2	81	20.6	5.0	6.8	3.7	38.42, 20.91	67	226
8	1954, 04, 30	13:02:36	39.28, 22.29	7.0	72	23.3	5.0	6.4	4.2	38.84, 21.82	64	40
9	1955, 07, 16	07:07:10	37.55, 27.05	6.9	47	37.5	5.0	6.5	13.9	37.43, 27.27	23	–
10	1956, 07, 09	03:11:40	36.64, 25.96	7.5	128	33.5	5.0	7.0	4.3	36.13, 26.37	68	327
11	1957, 04, 25	02:25:42	36.50, 28.60	7.2	50	21.3	5.0	6.8	3.2	37.18 27.44	128	126
12	1959, 11, 15	17:08:43	37.78, 20.53	6.8	46	4.9	4.5	5.9	2.4	38.44, 21.54	114	231
13	1960, 05, 26	05:10:11	40.63, 20.65	6.5	41	31.4	5.0	6.1	10.3	40.73, 20.57	13	–
14	1965, 07, 06	03:18:42	38.27, 22.30	6.3	43	10.5	4.5	5.4	3.9	38.34, 22.09	20	–
15	1967, 03, 04	17:58:09	39.20, 24.60	6.6	46	46.1	5.0	6.0	14.4	39.20, 24.12	41	89

Table I (*continued*).

N	Date	h:min:s	$\varphi^{\circ}_{N.}$ λ°_{E}	M	n	t_p	M_{min}	M_{13}	t_{13}	$\varphi^{\circ}_{N.}$ λ°_{E}	x	ξ
16	1967, 05, 01	07:09:02	39.47, 21.25	6.4	72	17.3	4.5	6.0	2.7	39.14, 21.09	39	20
17	1967, 11, 30	07:23:50	41.39, 20.46	6.3	41	13.9	4.5	5.5	6.9	41.51, 20.06	36	115
18	1968, 02, 19	22:45:42	39.50, 25.00	7.1	43	38.1	5.0	6.2	11.2	39.25, 24.64	41	48
19	1969, 03, 28	01:48:29	38.29, 28.57	6.6	47	17.2	4.5	5.6	3.4	38.22, 28.37	19	–
20	1970, 03, 28	21:02:23	39.16, 29.42	7.1	49	25.2	5.0	6.4	6.2	38.40, 28.96	93	25
21	1972, 05, 04	21:39:57	35.10, 23.60	6.5	64	21.3	4.5	5.6	8.5	35.01, 23.49	14	–
22	1972, 09, 17	14:07:15	38.30, 20.30	6.3	83	11.7	4.5	5.1	3.5	38.18, 20.52	24	–
23	1975, 03, 27	05:15:08	40.40, 26.10	6.6	70	21.2	4.5	5.8	5.2	39.89, 26.08	57	2
24	1976, 05, 11	16:59:45	37.40, 20.40	6.5	44	6.4	4.5	5.5	0.9	37.83, 20.88	64	222
25	1977, 09, 11	23:19:19	34.90, 23.00	6.3	95	26.7	4.5	5.8	15.4	34.92, 23.20	19	–
26	1978, 06, 20	20:03:21	40.61, 23.27	6.5	50	14.5	4.5	5.5	0.2	40.75, 23.23	16	–
27	1980, 07, 09	02:11:57	39.27, 22.83	6.5	99	22.5	4.5	6.0	8.7	38.84, 22.88	48	355
28	1981, 02, 24	20:53:37	38.07, 23.00	6.7	147	23.2	4.5	6.3	9.1	38.44, 22.91	42	169
29	1981, 12, 19	14:10:51	39.00, 25.26	7.2	526	32.0	4.5	6.8	9.8	39.05, 24.68	51	96
30	1982, 01, 18	19:27:25	39.78, 24.50	7.0	351	13.1	4.3	6.4	3.3	39.37, 23.80	75	53
31	1983, 01, 17	12:41:31	38.10, 20.20	7.0	438	13.0	4.5	6.5	4.6	38.50, 20.83	71	231

Table I (*continued*).

N	Date	h:min:s	φ°_{N}, λ°_{E}	M	n	t_p	M_{min}	M_{13}	t_{13}	φ°_{N}, λ°_{E}	x	ξ
32	1983, 07, 05	12:01:27	40.30, 27.20	6.4	58	29.5	4.5	5.9	7.0	39.84, 27.05	53	14
33	1984, 06, 21	10:43:43	35.40, 23.30	6.2	41	6.5	4.5	5.4	2.4	35.37, 23.12	16	–
34	1986, 09, 13	17:24:34	37.05, 22.11	6.0	56	19.7	4.3	5.2	1.2	37.01, 21.91	18	–
35	1988, 10, 16	12:34:04	37.91, 21.06	6.0	59	4.8	4.3	5.3	0.3	38.08, 20.68	38	120
36	1990, 06, 16	02:16:20	39.30, 20.60	6.0	54	4.5	4.0	5.1	1.8	39.28, 20.65	5	–
37	1990, 07, 09	11:22:16	34.80, 26.72	5.5	44	20.5	4.5	5.0	6.9	34.91, 26.80	15	–
38	1990, 12, 21	06:57:43	40.92, 22.36	6.0	49	24.0	4.3	5.2	5.5	40.84, 22.47	13	–
39	1992, 01, 23	04:24:19	38.40, 20.57	5.6	45	3.1	4.0	4.9	0.4	38.22, 20.58	20	–
40	1992, 04, 30	11:44:40	35.10, 26.60	6.1	226	22.3	4.3	5.6	7.3	35.13, 26.51	9	–
41	1992, 11, 06	19:08:10	38.19, 27.05	6.2	128	36.8	4.5	5.8	17.3	38.14, 27.14	10	–
42	1993, 08, 26	10:03:56	36.75, 28.06	5.6	41	21.6	4.3	5.1	8.7	36.78, 27.99	7	–
43	1994, 02, 25	02:30:50	38.76, 20.56	5.5	45	8.1	4.0	4.9	2.9	38.69, 20.56	7	–
44	1994, 04, 16	23:09:34	37.36, 20.63	5.5	43	7.3	4.3	4.9	1.0	37.41, 20.77	12	–
45	1994, 09, 01	16:12:42	41.15, 21.20	6.1	45	25.6	4.5	5.5	4.9	41.15, 21.05	12	–
46	1995, 05, 13	08:47:17	40.16, 21.67	6.6	42	19.4	5.0	6.0	3.3	39.14, 20.91	131	30
47	1995, 06, 15	00:15:49	38.37, 22.15	6.4	244	11.5	4.0	5.8	2.2	38.42, 21.58	50	96

Table I (*continued*).

N	Date	h:min:s	φ°_{N}, λ°_{E}	M	n	t_p	M_{min}	M_{13}	t_{13}	φ°_{N}, λ°_{E}	x	ξ
48	1996, 08, 05	22:46:43	40.05, 20.66	5.7	47	14.6	4.5	5.3	6.0	40.06, 20.57	7	–
49	1997, 10, 13	13:39:40	36.45, 22.16	6.4	41	10.8	4.5	5.2	6.1	36.57, 21.76	38	111
50	1997, 11, 14	21:38:52	38.73, 25.91	5.8	121	31.8	4.3	5.4	9.1	38.91, 26.00	22	–
51	1997, 11, 18	13:07:41	37.58, 20.57	6.6	143	13.9	4.5	6.1	5.4	37.81, 21.06	51	239
52	1999, 09, 07	11:56:51	38.06, 23.54	5.9	65	16.7	4.0	5.2	5.3	38.24, 23.15	40	119

The selection of the strong earthquakes for which preshock activity is investigated in this paper is based: a) on the available complete data mentioned above; b) on the observation that the duration of the accelerating seismicity is usually of the order of a few decades and, c) on the condition that each one of them is a mainshock (not an aftershock or a foreshock of a larger shock) and was preceded by at least 40 known smaller shocks (preshocks) in the critical area. There are 52 mainshocks, shown in fig. 1, that fulfil these criteria. For these events the code number (N), dates, epicentre coordinates and magnitudes are listed on the first four columns of table I. These mainshocks belong to five different sets, which consist of all such mainshocks, which have occurred in this area since 1930 with $M \geq 7.0$ (15 mainshocks), since 1950 with $6.9 \geq M \geq 6.8$ (2 mainshocks), since 1960 with $6.7 \geq M \geq 6.3$ (20 mainshocks), since 1981 with $6.2 \leq M \leq 6.0$ (7 mainshocks) and since 1990 with $5.9 \geq M \geq 5.5$ (8 mainshocks), respectively. The minimum number of preshocks is chosen to be relatively high (= 40), in order to achieve the highest accuracy in the derived relations, although smaller samples can also give good results.

The following relation between the seismic energy, E, and the moment magnitude, M, of shocks has been used (Papazachos and Papazachos, 2000) to calculate the Benioff strain (eq. 1.1):

$$\log E = 1.5M + 4.7 \qquad (2.1)$$

where E is measured in Joule.

An algorithm to identify regions of accelerating Benioff strain before mainshocks and to determine the parameters (A, B, m) of relation (1.2) has been developed and explained in detail in a previous work (Papazachos and Papazachos, 2000). According to this algorithm, preshocks included in an elliptical region centred at the epicentre of the mainshock are considered and the curvature parameter, C (ratio of the root-mean-square error of the power-law fit to the corresponding linear fit error), defined by Bowman *et al.* (1998), is calculated. This is repeated for several values of the azimuth, z (*e.g.*, in steps of 10°), of the length of the large ellipse axis, a (*e.g.*, in steps of 10 km), of the ellipticity e and of the starting time from when the accelerated seismicity period starts (*e.g.*, in 1 year steps). The solution (z, e, a, t_p, A, B, m) for which C has a minimum value, C_{min}, is adopted in the present paper as the final solution.

A critical region is not always uniquely defined for a mainshock, since it can be observed that other elliptical regions (with different orientation and ellipticity but with almost the same

Table II. Information on the parameters of the model used in the present paper for the fifty-two sequences. The code number, N, corresponds to the code number of table I. A (in 10^9 Joule$^{1/2}$), B (in 10^8 Joule$^{1/2}$/yr) and m are the parameters of relation (1.2). C is the curvature parameters, z (in degrees) is the azimuth of the maximum axis of the ellipse, e is its ellipticity, R (in km) is the radius of the circle which has an area equal to the corresponding ellipse, S_r (in Joule$^{1/2}$ per yr) is the rate of Benioff strain in each elliptical region, s_r (in Joule$^{1/2}$ per year and per 10000 km^2) is the rate of the Benioff strain per unit area, and P is a compatibility measure of empirical relations proposed in the present paper.

N	A	B	m	C	z	e	R	$\log S_r$	$\log s_r$	P
1	0.17	0.53	0.36	0.42	160	0.95	218	6.88	5.73	0.54
2	0.19	0.53	0.40	0.38	90	0.90	197	7.17	6.08	0.37
3	0.17	0.71	0.30	0.47	150	0.90	191	7.26	6.22	0.42
4	0.19	0.31	0.59	0.53	50	0.95	195	7.11	6.09	0.34
5	0.15	0.39	0.37	0.28	150	0.90	171	6.65	5.90	0.35
6	0.31	0.64	0.45	0.44	0	0.90	223	7.01	5.82	0.40
7	0.34	1.30	0.31	0.51	10	0.90	256	7.33	6.23	0.35
8	0.26	0.89	0.34	0.34	80	0.95	179	7.12	6.13	0.62
9	0.19	0.31	0.50	0.45	140	0.95	137	6.67	5.89	0.29
10	0.59	0.91	0.53	0.29	20	0.70	271	7.27	5.91	0.48
11	0.26	0.99	0.32	0.45	130	0.95	262	7.08	5.90	0.61
12	0.10	0.42	0.51	0.49	40	0.95	147	7.11	6.46	0.44
13	0.14	0.29	0.44	0.45	140	0.95	116	6.62	6.00	0.55
14	0.05	0.19	0.41	0.50	130	0.95	99	6.56	6.07	0.41
15	0.13	0.24	0.44	0.41	70	0.70	120	6.43	5.77	0.58
16	0.10	0.35	0.36	0.35	50	0.90	98	6.53	6.06	0.41
17	0.05	0.21	0.36	0.60	120	0.95	99	6.44	5.94	0.42
18	0.17	0.61	0.28	0.30	20	0.95	167	6.58	5.64	0.47
19	0.07	0.49	0.14	0.26	30	0.95	114	6.51	5.90	0.29
20	0.20	0.80	0.28	0.28	10	0.90	193	6.90	5.97	0.72
21	0.09	0.21	0.44	0.39	20	0.95	99	6.27	5.82	0.27
22	0.07	0.22	0.46	0.46	100	0.95	88	6.88	6.59	0.35
23	0.10	0.35	0.33	0.63	160	0.95	148	6.57	5.74	0.42
24	0.05	0.27	0.35	0.22	40	0.95	93	6.76	6.53	0.40
25	0.11	0.15	0.61	0.58	130	0.95	94	6.22	5.80	0.52
26	0.06	0.39	0.17	0.28	30	0.95	116	6.66	6.04	0.48
27	0.12	0.34	0.40	0.64	0	0.95	99	6.68	6.19	0.41
28	0.20	0.65	0.37	0.50	170	0.95	124	6.72	6.03	0.26
29	0.74	1.30	0.51	0.50	80	0.50	212	7.02	5.87	0.40
30	0.34	1.10	0.45	0.50	70	0.95	185	7.17	6.14	0.55
31	0.46	0.80	0.68	0.51	40	0.95	218	7.22	6.27	0.47
32	0.08	0.18	0.45	0.38	20	0.95	113	6.58	5.98	0.36
33	0.05	0.17	0.51	0.47	110	0.95	92	6.45	6.03	0.32
34	0.04	0.12	0.42	0.25	0	0.90	77	6.35	6.07	0.65

Table II *(continued)*.

N	A	B	m	C	z	e	R	$\log S_r$	$\log s_r$	P
35	0.04	0.26	0.34	0.33	120	0.90	58	6.71	6.70	0.27
36	0.03	0.13	0.57	0.66	90	0.60	67	6.40	6.25	0.31
37	0.03	0.05	0.63	0.45	30	0.95	41	5.78	6.05	0.29
38	0.04	0.08	0.47	0.39	170	0.70	66	5.80	6.66	0.42
39	0.02	0.12	0.50	0.47	140	0.70	56	6.90	6.91	0.32
40	0.17	0.24	0.63	0.29	130	0.70	80	6.38	6.08	0.25
41	0.13	0.17	0.56	0.67	140	0.95	98	6.44	5.96	0.32
42	0.03	0.06	0.55	0.59	30	0.95	39	5.76	6.08	0.26
43	0.02	0.05	0.66	0.63	70	0.80	36	6.26	6.66	0.31
44	0.03	0.09	0.63	0.35	150	0.90	49	6.42	6.55	0.30
45	0.05	0.07	0.62	0.28	110	0.95	69	5.91	5.74	0.27
46	0.12	0.23	0.56	0.53	20	0.95	148	6.98	6.14	0.39
47	0.14	0.31	0.59	0.42	100	0.95	90	6.80	6.39	0.42
48	0.05	0.16	0.40	0.62	100	0.95	54	6.20	6.23	0.29
49	0.05	0.19	0.39	0.37	100	0.80	93	6.56	6.13	0.34
50	0.08	0.08	0.66	0.59	30	0.90	67	5.93	5.78	0.34
51	0.17	0.29	0.67	0.54	50	0.95	103	6.81	6.45	0.35
52	0.04	0.08	0.53	0.69	120	0.90	72	6.21	5.99	0.52

area) may also fulfil the criteria required by the method (minimum value of the curvature C within the error limits, etc.). The main preshock clusters, however, are included in all these different elliptical regions. For this reason, the mean epicentre of preshocks of a certain mainshock can be reliably determined.

Table II gives the parameters (A, B, m, C, z, e, R) of the model described above for each of the fifty-two sequences. The logarithms of the Benioff strain rate, S_r, for the whole critical region and of the same rate, s_r per 10000 km^2, are also given. The mean values of the parameters m and C are 0.46 ± 0.13 and 0.45 ± 0.12, respectively, while the ellipticity values are usually very high (larger than 0.8). The values of R vary between 33 km and 262 km, while the preshock time t_p ranges between 3 and 46 years with an average of 20 years.

The calculated values of the parameters, A, B, m of the relation (1.2) hold for ellipses centred at the epicentre of the mainshock. For an ensuing mainshock, however, this epicentre is not known but the mean epicentre of preshocks is known. For this reason, we repeated the calculations of these parameters for ellipses centred at the mean preshock epicentre. The mean ratios of the new values to the old ones were found equal to 0.97 ± 0.14 for A, 0.96 ± 0.10 for B and 1.01 ± 0.13 for m, which indicates that the model can also be applied for ellipses which are centred at the mean preshock epicentre.

3. Relations between the parameters of the model

The values of the radius, R (in km), listed in table II are plotted *versus* the magnitude, M, of the mainshock in fig. 2. The data are fitted, in the least squares sense, using the relation:

$$\log R = 0.41\, M - 0.64 \qquad (3.1)$$

with a correlation coefficient equal to 0.97 and standard deviation equal to 0.05. This relation is

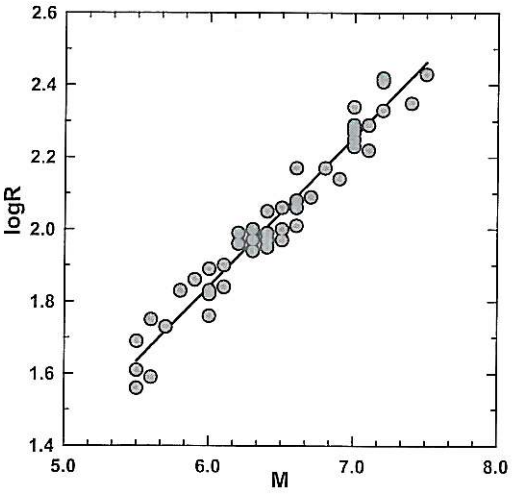

Fig. 2. Relation between the radius, R (in km), of the circle which has an area equal to the elliptical critical region and the magnitude, M, of the mainshock.

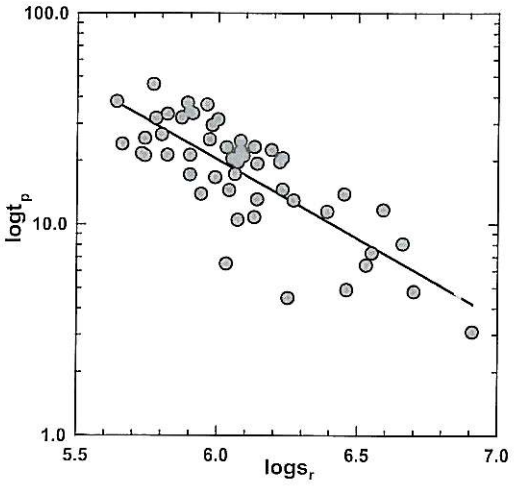

Fig. 3. Relation between the duration of a preshock sequence, t_p (in years), and the Benioff strain rate, s_r (in Joule$^{1/2}$ per year and per 10000 km^2).

almost identical with the one derived previously by the use of a smaller sample of data (Papazachos and Papazachos, 2000) and in very good agreement with data concerning other regions (Bowman *et al.*, 1998). This indicates that relation (3.1) is of global validity and holds at least for earthquakes with $M \geq 5.5$.

Figure 3 shows a plot of the logarithm of the preshock time, t_p (in years), as a function of the rate of the Benioff strain, s_r (in Joule ½ per year and per 10000 km^2), on the basis of the corresponding data given in tables I and II. Using these data the following relation was defined:

$$\log t_p = 5.81 - 0.75 \log s_r \qquad (3.2)$$

with a correlation coefficient equal to 0.79 and a standard deviation equal to 0.17.

From tables I and II, we can derive that $\log(A/t_p)/\log S_r = 1.020$ with a standard deviation equal to 0.030. Therefore, the relation

$$A = S_r t_p \qquad (3.3)$$

which has been previously proposed also applies to the new larger data sample.

Figure 4 shows a plot of the $\log B$ against the magnitude of the mainshock. The data are fitted by the relation

$$\log B = 0.64 M + 3.27 \qquad (3.4)$$

with a correlation coefficient equal to 0.91 and a standard deviation equal to 0.16. The form of this relation is in agreement with Brehm and

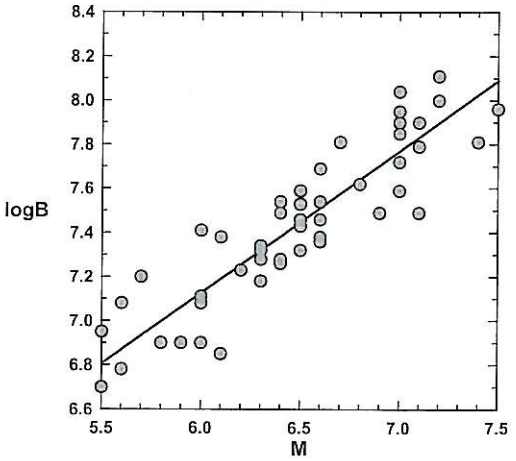

Fig. 4. Relation between the parameter, B (in Joule$^{1/2}$ per year), and the magnitude, M, of the mainshock.

Braile (1999) who found a linear relation between log$B$ and the logarithm of the seismic moment of the mainshock.

Figure 5 shows a plot of the magnitude of the mainshock against the average magnitude, M_{13}, of the three largest preshocks. A linear relation

$$M = 0.85\,M_{13} + 1.52 \qquad (3.5)$$

is also defined with a correlation coefficient equal to 0.92 and a standard deviation equal to 0.21. A similar relation was proposed by Evison and Rhoades (1997) for precursory earthquake swarms.

From table I we find that the mean ratio of the average time difference, t_{13}, of the three largest preshocks from the origin time of the mainshock to the total duration, t_p, of the preshock sequence is 0.29 with a standard deviation equal to 0.13, hence

$$t_{13} = 0.29\,t_p. \qquad (3.6)$$

Equation (1.2) indicates that the largest preshocks occur mainly during the second phase of a preshock sequence, while the mean value of t_{13} is 5.9 ± 3.9 years.

Relations (3.1), (3.2), (3.3), (3.4) and (3.5) are similar to the ones previously derived by the use of a smaller sample of data (Papazachos and Papazachos, 2000, 2001), although relations (3.2) and (3.4) are slightly modified. In any case, the proposed relations in the present paper are based on a large number of sequences (52 sequences), each sequence includes a large number of preshocks (between 40 and 526) and the quantities involved cover a relatively wide interval range (*e.g.*, the magnitudes range between 5.5 and 7.5), hence they must be considered more reliable than the ones previously defined.

In order to compare the obtained results regarding the R, t_p, A, B and M_{13} values estimated for each earthquake with the relations previously determined, the probability of each obtained parameter was calculated. For this reason, each model parameter was estimated with respect to its expected value, assuming that the deviations of each parameter follow a Gaussian distribution. For example, for the equivalent radius, R, the quantity $Z_R = (\log R\text{-}a\text{-}b^{*}M)/\sigma_{\log R})$ was used as the normalized variable and the corresponding Gaussian probability, $P_{\log R} = \mathrm{errf}(Z_R)$, was determined, where errf() is the error function. Finally the quantity

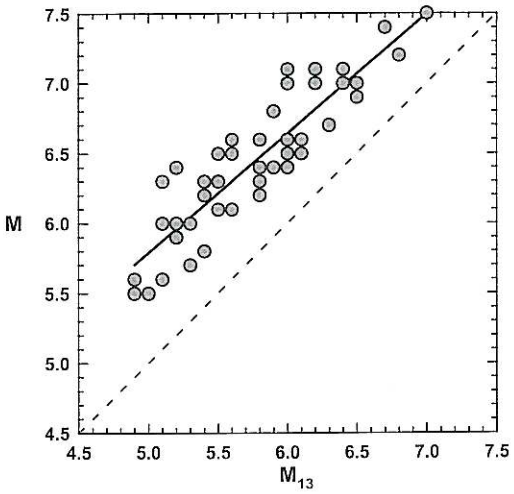

Fig. 5. Relation between the magnitude of the mainshock, M, and the mean magnitude, M_{13}, of the three largest preshocks.

$$P = P_{\log R} + P_{\log t_p} + P_{\log(A/t_p)} + P_{\log B} + P_{M13} \qquad (3.7)$$

was used as a measure of the agreement of the determined model parameters with the «global» relations previously determined. In general the probability product is a more appropriate measure of the probability for the obtained R, t_p, A, B and M_{13} values. However, such a definition would lead to practically zero-probabilities if one of these parameters exhibited significant deviations from the expected values, given the low tolerance of the Gaussian distribution to outliers. Since we did not want to exclude such solutions, the simpler and more robust definition to outliers given in eq. (3.7) was preferred. It must be noted that P should not be regarded as a measure of the quality of the solution but a simple quantification of the compatibility of the obtained R, t_p, A, B and M_{13} values for each event with the values determined from eqs. (3.1)-(3.5). This compatibility measure, P, which is given in the last column of table II, varies between 0.25 and 0.71.

4. Locations of preshocks

Although every critical region determined by the methodology applied in the present paper has a symmetrical shape with respect to the epicenter of the corresponding mainshock, since this region is an ellipse centered at the mainshock epicenter, the mean epicenter of preshocks is at some distance from the mainshock epicenter as can be seen in table I. We have examined the location of this mean epicenter of preshocks, with respect to the epicenter of the mainshock and its dependence on the dimensions of the preshock region and tectonic factors.

Figure 6 shows a plot of the logarithm of the distance, x (in km), between the mean preshock epicenter and the mainshock epicenter against the magnitude of the mainshock. A linear relation was fitted in the data, having the form

$$\log x = 0.49M - 1.66 \qquad (4.1)$$

with a correlation coefficient equal to 0.73 and a standard deviation equal to 0.24. This relation, in combination with the relation (3.1), shows that the distance, x, between the mainshock epicenter and the mean preshock epicenter increases with the size of the critical region. It is of interest to note that relation (1.1) gives values of x almost equal to the fault length for the corresponding mainshock magnitude (Papazachos and Papazachou, 1997).

From the azimuths, ξ (listed in table I), of the vectors x that connect the mean preshock epicenter with the mainshock epicenter and have lengths $x \geq 30$ km, we can arrive at certain conclusions that are of tectonic significance (for smaller distances the azimuths are not reliable). Hence, most of the mainshocks for which $x \geq 30$ km are located along the boundaries of the Aegean plate (fig. 1). According to the orientation of the vector x we can define three main regimes.

The first regime is located in the southwestern boundary of the Aegean plate (Ionian Islands), which is the most active part of the investigated region and includes the epicenter of five strong earthquakes (with code numbers 7, 12, 24, 31, 51 in table I). The mean azimuth of the vector x for these five cases is $\xi = 230° \pm 6°$.

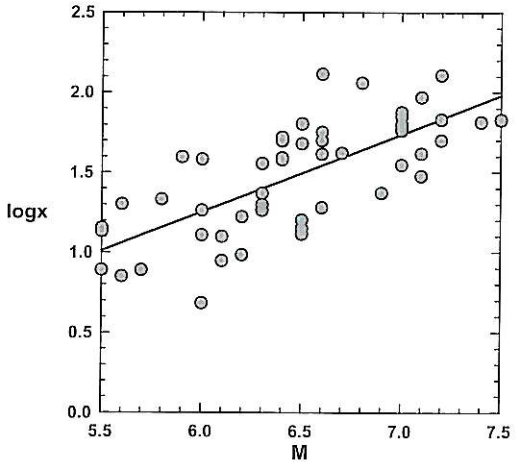

Fig. 6. Relation between the distance, x (in km), of the mean epicenter of preshocks from the mainshock epicenter and the magnitude M of the mainshock.

It shows that this vector has a southwestward direction, which is the direction of motion of the Aegean plate in this region (Papazachos, 1999). It probably indicates that the strong earthquakes in the Cephalonia-Zante area, which are generated by dextral and/or thrust faulting, are preceded by preshocks which are mainly located within the Aegean plate and are generated by normal or strike slip faulting. This can be interpreted by assuming that expansion of the Aegean plate precedes its overthrusting on the Mediterranean lithosphere along its southwestern boundary.

The second regime covers the northern boundary of the Aegean plate (Central Greece-Northern Aegean-Northwest Anatolia) and includes the epicenters of twelve strong earthquakes (with code numbers 1, 6, 8, 15, 16, 18, 20, 23, 27, 29, 30, 32 in table I). The mean azimuth of the vector x for these twelve cases is $\xi = 34° \pm 31°$, that is, this vector is almost parallel to the northern boundary of the Aegean plate but opposite to the direction of motion of this plate. This observation shows that strong earthquakes along the northern boundary of the Aegean plate are preceded by preshocks, which are mainly located southwestward in respect to the epicenters of the mainshock. This probably

suggests that strike-slip (dextral) or normal fault ruptures, which generate strong earthquakes along the northern boundary of the Aegean plate, are preceded by preshock deformation of this plate which takes mainly place southwestward of these ruptures.

The third regime includes five mainshocks (with code numbers 3, 28, 47, 49, 52 in table I) and covers the southwestern part of the Aegean area (Peloponnese, etc.). The mean azimuth of the vector x for these five cases is $129° \pm 27°$. It means that the mainshocks in this region are preceded by preshocks, which are mainly located to the northwest. No obvious tectonic explanation for this property can be made at the moment.

5. Discussion

The results of the present paper are of theoretical importance because they give useful information concerning the behavior of parts of the lithosphere before the generation of a large earthquake. Of equal or even higher importance is the consequence of these results on the problem of prediction of such large earthquakes. For this reason some relative discussion can be of interest from a practical point of view.

If a relatively large number of preshocks of an ensuing mainshock are known, their mean epicenter can be determined and it can be taken as an initial center of the ellipses which are used to fit the data by the proposed algorithm. This approach is quite safe because the calculated parameters of relation (1.2) do not vary significantly if we use this point as center of the ellipses instead of the mainshock epicenter. On the other hand, an estimation of the area covered by the epicenters of preshocks can be used to calculate an initial value of the mainshock magnitude (relation (3.1)) and of A ($= A_m + A_p$) and B (relation (3.4)). Initial values can then be calculated for the parameter m and for the origin time, t_c, of the mainshock by fitting relation (1.2) to the available data.

Having initial values for the parameters of relation (1.2) an iterative procedure can be applied to calculate the final magnitude and origin time for the expected mainshock, as well as the final location of the mean preshock epicenter. This procedure must be based on a modified version of the algorithm proposed above, using a similar procedure of minimization of the curvature parameter C and the constraints imposed by relations (3.1)-(3.6).

The elliptical regions determined by this procedure are centered at the mean epicenter of preshocks. The epicenter of the mainshock is expected to be located within a distance that is given by the relation (4.1). This relation gives acceptable uncertainties for the mainshock epicenter ($x = 11$ km for $M = 5.5$, $x = 33$ km for $M = 6.5$ and $x = 104$ km for $M = 7.5$) since these uncertainties are of the same order with the fault length of the corresponding earthquakes.

The previously described procedure or any similar procedure based on the results of the present paper must be considered a working hypothesis to be tested. Such test for an *a posteriori* prediction of past strong earthquakes is already underway. There are, however, additional problems, which must be solved before this methodology is applied for prediction of future large earthquakes. One such problem is the possibility that a region can be in a critical state for a certain time interval without ending in a mainshock. We believe, however, that the fact that all 52 mainshocks examined in the present paper were preceded by accelerating seismic deformation in elliptical regions centered at the mainshock epicenter is of great importance for practical earthquake prediction. Furthermore, the identified relations between the main quantities involved in eq. (1.2) confirm the applicability in practical problems of the theoretical background behind the pattern of accelerated seismic energy release prior to large events.

REFERENCES

ALLEGRE, C.J. and J.L. Le MOUËL (1994): Introduction of scaling techniques in brittle failure of rocks, *Phys. Earth Planet. Inter.*, **87**, 85-93.

ANDERSEN, J.V., D. SORNETTE and K.T. LEUNG (1997): Tri-critical behavior in rupture induced by disorder, *Phys. Rev. Lett.*, **78**, 2140-2143.

BOWMAN, D.D., G. QUILLON, C.G. SAMMIS, A. SORNETTE and D. SORNETTE (1998): An observational test of the critical earthquake concept, *J. Geophys. Res.*, **103**, 24359-24372.

BREHM, M.J. and L.W. BRAILE (1999): Refinement of the modified time - to failure method for intermediate - term earthquake prediction, *J. Seismology*, **3**, 121-138.

BUFE, C.G. and D.J. VARNES (1993): Predictive modeling of seismic cycle of the Great San Francisco Bay Region, *J. Geophys. Res.*, **98**, 9871-9883.

EVISON, F.F. and D.A. RHOADES (1997): The precursory earthquake swarm in New Zealand., *N. Z. J. Geol. Geophys.*, **40**, 537-547.

KNOPOFF, L., T. LEVSHINA, V.J. KELLIS-BOROK and C. MATTONI (1996): Increased long-range intermediate-magnitude earthquake activity prior to strong earthquakes in California, *J. Geophys. Res.*, **101**, 5779-5796.

MARGARIS, B.N. and C.B. PAPAZACHOS (1999): Moment-magnitude relations based on strong-motion records in Greece, *Bull. Seismol. Soc. Am.*, **89**, 442-445.

MOGI, K. (1969): Some features of the recent seismic activity in the near Japan, 2, activity before and after great earthquakes, *Bull. Earthquake Res. Inst. Univ. Tokyo*, **47**, 395-417.

PAPADOPOULOS, G.A. (1986): Long term earthquake prediction in the Western Hellenic arc, *Earthquake Predict. Res.*, **4**, 131-137.

PAPAZACHOS, C.B. (1999): Seismological and GPS evidence of the Aegean-Anatolia interaction, *Geophys. Res. Lett.*, **26**, 2653-2656.

PAPAZACHOS, B.C. and C.B. PAPAZACHOU (1997): *The Earthquakes of Greece* (Ziti Editions, Thessaloniki), pp. 304.

PAPAZACHOS, B. and C. PAPAZACHOS (2000): Accelerated preshock deformation of broad regions in the Aegean area, *Pure Appl. Geophys.*, **157**, 1663-1681.

PAPAZACHOS, C. and B. PAPAZACHOS (2001): Estimates of model parameters for the accelerating preshock crustal deformation in regions of the Aegean area, *J. Seismology* (submitted).

PAPAZACHOS, B.C., A.A. KIRATZI and B.G. KARAKOSTAS, (1997): Toward a homogeneous moment magnitude determination in Greece and surrounding area, *Bull. Seismol. Soc. Am.*, **87**, 474-483.

PAPAZACHOS, B.C., P.E. COMNINAKIS, G.F. KARAKAISIS, B.G. KARAKOSTAS, CH.A. PAPAIOANNOU, C.B. PAPAZACHOS and E.M. SCORDILIS (2000): A catalogue of earthquakes in Greece and surrounding area for the period 550BC-1999, *Publ. Geophys. Lab. Univ. Thessaloniki*, **1**, pp. 338.

RALEIGH, C.B., K. SIEH, L.R. SYKES and D.L. ANDERSON, (1982): Forecasting Southern California earthquakes, *Sciences*, **217**, 1097-1104.

SORNETTE, A. and D. SORNETTE (1990): Earthquake rupture as a critical point. Consequences for telluric precursors, *Tectonophysics*, **179**, 327-334.

SYKES, L.R. and S. JAUME (1990): Seismic activity on neighbouring faults as a long term precursor to large earthquakes in the San Francisco bay area, *Nature*, **348**, 595-599.

TOCHER, D. (1959): Seismic history of the San Francisco region, in San Francisco earthquakes of 1957, Edited by G.B. OAKESHOTT, *CDMG Spec. Rep. 57*, Cal. Div. Mines. Geol., Sacramento, 39-48.

VARNES, D.J. (1989): Predicting earthquakes by analyzing accelerating precursory seismic activity, *Pure Appl. Geophys.*, **130**, 661-686.